

# On the distinct observation of the moving triangle singularity

V.M.Kolybasov \*

Lebedev Physical Institute, 117924 Moscow, Russia

## Abstract

It is shown that nonzero orbital momentum in the vertex of secondary interaction in the triangle graph leads to a more clear picture corresponding to the moving complex singularity compared with the case of constant vertex. The peak in the distribution of the final particles invariant mass becomes narrower and its shift with momentum transfer more distinct. It opens the possibility to observe this picture experimentally.

*PACS:* 11.55.Bq; 24.50.+g; 25.10.+s

*Keywords:* Triangle mechanism; Moving singularity; Experimental observation.

The triangle mechanism (see Fig.1 graph) is one of the simplest mechanisms of direct nuclear interactions. It is very frequently used in the description of nuclear reactions. A characteristic graph of this type corresponds to a primary interaction (the right upper vertex) followed by secondary elastic or inelastic interaction (the lower vertex). The experimental determination of its contribution as well as separation of the kinematical regions of its domination would permit us to extract valuable and reliable information on nuclear structure and the off-shell amplitude of the “elementary” process in the lower vertex.

Until now very few cases are known when the dominant contribution of the triangle mechanism is seen. Let us point to the peak in pion spectrum from the capture of stopped kaons on the deuteron  $K^-d \rightarrow p\Lambda\pi^-$  [1] due to the triangle graph with  $N\Sigma$  intermediate state and the conversion  $N\Sigma \rightarrow p\Lambda$  [2]. Besides it is possible to mention anomalies in photonuclear interactions [3] and enhancements in two nucleon mass spectra near  $2m_N$  due to FSI [4]. On the other side, it is well known that the characteristic feature of the triangle graph in nuclear physics consists in so called moving complex triangle singularity. Its position in the invariant mass  $M$  of the lower group of final particles depends on the value  $q$  of three-momentum transfer from initial to final fast particles in the right vertex [5]. The distribution with respect to  $M$  depends on the value of  $q$ . It is a model-independent criterion of the dominant role of the graph [6]. Up to now this test was not used for the identification of the triangle mechanism. The estimations for the process  $pd \rightarrow pd\eta$  [7] and for several other processes with an intermediate  $\Delta$ -isobar [8] predict a clear picture of the moving singularity but there will be rather broad maxima in the  $M$  distributions with widths of the order of  $100 \div 200$  MeV.

Of course, the most distinct picture could be expected in the region of the excitation energy  $E_{\text{ex}} = M - (m_1 + m_2)$  of the order of nuclear binding energies and momentum transfer  $q$  of the order of nuclear Fermi-momenta. Here the complex triangle singularity comes close to the physical region and narrow peaks and background suppression could be anticipated. Moreover, the cross sections in this region are much larger. It is hindered by

the fact that Fig.1 triangle graph has also the threshold root singularity at  $E_{\text{ex}} = 0$  and usually it determines a picture of the spectrum at small  $E_{\text{ex}}$ . As we shall see below, the picture of the moving singularity get too smooth and hardly yields to observation.

However, the situation sharply varies if not the s-wave but p- or higher waves dominate in the amplitude of secondary interaction. The shape of the cusp singularity changes and it ceases to dominate at small  $E_{\text{ex}}$ . As will be shown below, the situation with observation of the moving triangle singularity is essentially improved and we can see very clear and unambiguous picture. Later on it will be illustrated on graphic examples. Yet at first we will develop a formalism for Fig.1 graph calculation with arbitrary nuclear form factor in  $A \rightarrow 1 + 3$  vertex and account of nonzero orbital momenta in the lower vertex.

Except the quantities  $M$ ,  $E_{\text{ex}}$  and  $\mathbf{q} = \mathbf{p}_x - \mathbf{p}_y$  (all momenta in lab. system), introduced earlier, we will also use the nuclear binding energy  $\varepsilon = m_1 + m_3 - m_A$  and the characteristic momentum  $\kappa$  in the nuclear vertex  $A \rightarrow 1 + 3$ :  $\kappa^2 = 2m_{13}\varepsilon$ , where  $m_{13}$  is the reduced mass of particles 1 and 3. We will usually consider nuclear reactions and take the particles A, 1 and 3 to be nonrelativistic. It is convenient to use the dimensionless variables  $\xi$  and  $\lambda$  [9,7], associated with  $M$  and  $q$ :

$$\xi \equiv \xi(M, q) = \frac{m_A}{2m_3\varepsilon} \left\{ \frac{m_1 q^2}{M^2 + q^2} + \frac{M^2 + m_1^2 - \mu^2}{\sqrt{M^2 + q^2}} - 2m_1 \right\}, \quad (1)$$

$$\lambda \equiv \lambda(M, q) = \frac{m_1^2}{M^2 + q^2} \frac{q^2}{\kappa^2}. \quad (2)$$

These expressions are valid in general case of relativistic particle 2. In the nonrelativistic case  $\xi$  is expresses only through  $M$ :

$$\xi \equiv \xi(M) = \frac{m_2}{m_3} \frac{m_A}{M} \frac{M - m_1 - m_2}{\varepsilon}. \quad (3)$$

In terms of these variables the triangle graph has a square root branching point at  $\xi = 0$  and logarithmic singularities at  $\xi = \lambda - 1 \pm i\sqrt{\lambda}$ .

Let us go to the estimation of Fig.1 graph for the case of arbitrary upper left (nuclear) and lower (secondary interaction) vertices. We will take the upper right (primary interaction) vertex to be constant, equivalent to factoring out its value in the triangle integral

at some point near the maximum of the integrand. Usually this means that we factor out the amplitude of the process  $x + 3 \rightarrow y + 2$  at the proper momentum transfer and at the energy corresponding to the interaction of particle  $x$  with particle 3 at rest. The amplitude of the graph has the form of a four-fold integral over the 4-momentum  $p$  of particle 3 [10]. The integration over the fourth component reduces to determining the residue in the pole of the propagator of particle 1. (Then neglected terms are of the order  $\sqrt{\varepsilon/m}$  or  $\varepsilon/\mu$  where  $m$  and  $\mu$  are nucleon and pion masses.) So in reality we have three-fold integral over  $\mathbf{p}$ , containing propagators of particles 2 and 3 and two nontrivial vertices. The nuclear vertex  $A \rightarrow 1 + 3$  together with the propagator of particle 3 corresponds to a nuclear wave function  $\Psi_l(p)Y_{lm}(\hat{\mathbf{p}})$ . The lower vertex can be represented as

$$\varphi_L(k)Y_{LM}^*(\hat{\mathbf{k}}) \quad (4)$$

where  $\mathbf{k}$  is the relative momentum of particles 1 and 2

$$\mathbf{k} = \mathbf{p} + \mathbf{Q}, \quad \mathbf{Q} = \frac{m_1}{m_1 + m_2}\mathbf{q}. \quad (5)$$

Here  $l$  and  $L$  are the orbital momenta of the nuclear vertex and the secondary interaction vertex. As for the latter, we deal here only with nontrivial part (4) of its amplitude which contains the dependence on  $\mathbf{k}$ . The most interesting phenomena appear in the  $M$  region not far from the threshold of the channel (1+2), i.e. for  $m_1 + m_2$  not far from  $M$ , where the dependence on  $\mathbf{k}$  is most important. Actually all vertices also contain spin parts (Clebsch - Jordan coefficients due, for example, to spin-orbital interaction), but these do not influence the integration procedure.

The propagator of particle 2 can be transformed to the form

$$2m_2E_2 - \mathbf{p}_2^2 + i\eta = -\frac{m_1 + m_2}{m_1}\{(\mathbf{p} + \mathbf{Q})^2 - 2m_{12}E_{ex} - i\eta\}. \quad (6)$$

Note that  $Q^2 = \lambda\kappa^2$ ,  $2m_{12}E_{ex} = \xi\kappa^2$ . The propagator (6) contains the same vector combination as in eq.(5) that is the relative momentum of particles 1 and 2. This is important for our formal transformations. This statement is valid also in the case of a relativistic particle 2

(see ref. [9]). The expression for the amplitude of the triangle graph of Fig.1 is proportional to

$$I_{\Delta} = \int d\mathbf{p} \frac{\Psi_l(p) Y_{lm}(\hat{\mathbf{p}}) \varphi_L(|\mathbf{p} + \mathbf{Q}|) Y_{LM}^*(\mathbf{p} + \mathbf{Q})}{(\mathbf{p} + \mathbf{Q})^2 - 2m_{12} E_{ex} - i\eta}. \quad (7)$$

Here  $E_{ex}$  can take positive as well as negative values.

Let us transform eq.(7) to coordinate space and use nuclear wave function in coordinate space  $\psi_l(r) Y_{lm}(\hat{\mathbf{r}})$ :

$$\Psi_l(p) Y_{lm}(\hat{\mathbf{p}}) = \int \psi_l(r') Y_{lm}(\hat{\mathbf{r}}') e^{i\mathbf{p}\mathbf{r}'} d\mathbf{r}'. \quad (8)$$

If the lower vertex were constant we would use one of the following relations to transform the denominator of eq.(7):

$$\frac{1}{\mathbf{k}^2 - \alpha^2 - i\eta} = \frac{1}{4\pi} \int \frac{e^{i\mathbf{k}\mathbf{r} + i\alpha r}}{r} d\mathbf{r}, \quad \frac{1}{\mathbf{k}^2 + \beta^2} = \frac{1}{4\pi} \int \frac{e^{i\mathbf{k}\mathbf{r} - \beta r}}{r} d\mathbf{r}. \quad (9)$$

Then simple calculation would lead to the result (for example if  $E_{ex} < 0$ )

$$I_{\Delta} = (2\pi)^3 i^l Y_{lm}(-\mathbf{Q}) \int_0^{\infty} dr r j_l(\sqrt{\lambda} \kappa r) \exp(-\sqrt{-\xi} \kappa r) \psi_l(r). \quad (10)$$

For the case  $E_{ex} > 0$  the quantity  $-i\sqrt{\xi}$  must be substituted for  $\sqrt{-\xi}$ .

For an arbitrary lower vertex we will apply a transformation to coordinate space which includes a new function  $f_L(r)$  which will be described later:

$$\frac{\varphi_L(k) Y_{LM}^*(\hat{\mathbf{k}})}{k^2 + \beta^2} = \int Y_{LM}^*(\hat{\mathbf{r}}) f_L(r) e^{-i\mathbf{k}\mathbf{r}} d\mathbf{r}. \quad (11)$$

Then straightforward but tedious calculations lead to the result

$$I_{\Delta} = (2\pi)^3 \sqrt{4\pi(2l+1)} (-1)^l \sum_{T,t} i^T C_{10L0}^{T0} C_{lmTt}^{LM} Y_{Tt}^*(-\hat{\mathbf{Q}}) \cdot \int_0^{\infty} dr r^2 j_T(Qr) \psi_l(r) f_L(r) \quad (12)$$

where  $j_T$  is a spherical Bessel function. The nontrivial part of  $I_{\Delta}$ , which will be denoted as  $\mathcal{M}$

$$\mathcal{M} = \int_0^{\infty} dr \cdot r^2 j_T(Qr) \psi_l(r) f_L(r), \quad (13)$$

contains one-fold integral with radial part of nuclear wave function and function  $f_L(r)$  associated with the lower vertex of the triangle graph of Fig.1. Here  $T$ ,  $l$  and  $L$  must obey the triangle rule. The relative weights of terms with different  $T$  in the final results for the cross section, polarizations etc. will depend not only on factors in eq.(12) but also on the spin structure of all vertices in the triangle graph.

Let us turn to eq.(11). Inverse transformation gives

$$f_L(r) = \frac{i^L}{2\pi^2} \int_0^\infty \frac{\varphi_L(k) j_L(kr)}{k^2 + \beta^2} k^2 dk. \quad (14)$$

Various choices of this function are described in ref. [9]. Here we consider only one kind chosen such as to give a correct behavior of the amplitude for the case of arbitrary orbital momenta in the near-threshold region:

$$\varphi_L(k) = C k^L. \quad (15)$$

Then for example

$$f_0(r) = \frac{C e^{-\beta r}}{4\pi r} = -\frac{C\beta}{4\pi} h_0^{(1)}(i\beta r). \quad (16)$$

In the general case, a minimum account of the centrifugal barrier requires

$$f_L(r) = (-1)^{(L+1)} C \frac{\beta^{L+1}}{4\pi} h_L^{(1)}(i\beta r), \quad (17)$$

where  $h_L^{(1)}$  is the spherical Hankel function of the first class. Expressions (11), (14), (16), (17) correspond to  $\xi < 0$  when  $\beta = \sqrt{-\xi}\kappa$ . For the case  $\xi > 0$  the quantity  $\beta$  in these expressions must be changed into  $-i\gamma$  where  $\gamma = \sqrt{\xi}\kappa$ .

The formula (13) enables us to carry out numerical estimations in a simple way. Here we will show the results of concrete calculations for several cases with s- and p- orbital momenta. For s-wave nuclear wave functions we used the deuteron function in Paris potential as well as the wave function in Gauss parametrization  $\psi(r) \sim \exp(-p_0^2 r^2/2)$ . For the p-wave we used a p-wave Gauss function  $\psi(r) \sim r \exp(-p_0^2 r^2/2)$  as well as a ‘‘quasi-Hulten’’ p-wave function of the form

$$\psi(r) \sim \left( \frac{1}{\kappa r} + \frac{1}{\kappa^2 r^2} \right) \left( e^{-\kappa r} - 3e^{-(\kappa+\rho)r} + 3e^{-(\kappa+2\rho)r} - e^{-(\kappa+3\rho)r} \right) \quad (18)$$

which has correct asymptotic behavior at  $r \rightarrow 0$  and  $r \rightarrow \infty$ .

Fig.2 shows the results for  $|\mathcal{M}|^2$  for the case of the deuteron with Paris wave function: a) for s-wave lower vertex and b) for p-wave lower vertex. In the latter case there is now a distinctive and pronounced systematic pattern in which the maximum of the distribution moves to larger values of  $\xi$  with increasing  $\lambda$ . For s-wave Gauss function the pattern are close to the deuteron case. Fig.3 illustrates the corresponding effect for the case of p-wave Gauss nuclear function with  $p_0 = 0.75\kappa$  (it corresponds to  $^{12}\text{C}$ ). Again the picture is more distinct for the case of p-wave lower vertex. The p-wave “quasi-Hulten” function (18) gives similar results. These calculations were done with the amplitude of lower vertex of the Fig.1 graph in the form (22). Introduction of cut-off factors (see ref. [9]) does not lead to the qualitative changes. We see that the cases with the p-wave lower vertex open the possibility to observe the picture of the moving triangle singularity experimentally. Up to now this picture has not been exploited for the identification of the triangle mechanism.

In conclusion it can be said that we have first derived the simple and transparent formulas (12)-(14) for the triangle graph with arbitrary orbital momenta in the nuclear vertex and in the vertex of secondary interaction. The amplitude is represented in the form of one-fold integral in coordinate space. It is well suitable for numerical calculations due to the exponential decrease of the nuclear wave function.

We then have pointed out that nonzero orbital momenta in the vertices have an important effect on the shape of experimental distributions. This idea is supported by the graphical results. The corresponding singularity manifests itself much more distinctly and sharply than for the case with  $L = 0$ . The experimental demonstration of this effect requires favourable situations. This is not easy, since the most interesting region is located close to the threshold for particles  $1 + 2$ , where the p-wave amplitude is normally suppressed by the barrier. One interesting example is  $\bar{N}N$ -interaction in the final state for which the p-wave is greatly enhanced at low energies and can be separated by the choice of particular channels [11]. A second example is the  $\pi N$ -interaction which is dominated by p-wave part from rather small

energies.

The author is indebted to Prof. O.D.Dalkarov, T.E.O.Ericson and I.S.Shapiro for discussions. He also appreciate the hospitality of The Svedberg Laboratory of the Uppsala University where a part of this investigation was done.

## References

- [1] T.H.Tan, Phys.Rev.Lett. 23 (1969) 395.
- [2] R.H. Dalitz, Strange particles and strong interactions, Oxford University Press, 1962.  
A.E.Kudryavtsev, JETP Letters 14 (1971) 137.  
G.Torek, A.Gal, J.M.Eisenberg, Nucl.Phys. A362 (1981) 405.
- [3] P.E.Argan et al., Phys.Rev.Lett. 41 (1978) 86.  
G.Audit et al., Nucl.Phys. A614 (1997) 461.
- [4] M.L.Goldberger, K.W.Watson, Collision Theory, John Wiley & Sons, N.Y.–London–Sidney, 1964.
- [5] L.D.Blokhintsev, E.I.Dolinsky and V.S.Popov, JETP 43 (1962) 2291 (Sov. Phys. JETP 15 (1962) 1136).  
B.N.Valuev, JETP 47 (1964) 649. V.V.Anisovich, L.G.Dakhno, JETP 46 (1964) 1152.
- [6] E.I.Dubovoj and I.S.Shapiro, JETP 51 (1966) 1251 (Sov. Phys. JETP 24 (1967) 839).
- [7] V.M.Kolybasov, Phys.Lett. B439 (1998) 251. V.M.Kolybasov, Preprint of Lebedev Physical Institute no.31, Moscow, 1995.
- [8] O.D.Dalkarov and V.M.Kolybasov, Sov. J. Nucl. Phys. 18 (1974) 416.  
V.M.Kolybasov, in Proc. Int. Symposium “Dubna Deuteron-95”, JINR, Dubna, 1996, p.70.



- [9] V.M.Kolybasov, Preprint of Lebedev Physical Institute no.42, Moscow, 1997. Physics of Atomic Nuclei, in print.
- [10] I.S.Shapiro, in Selected topics in nuclear theory, IAEA, Vienna, 1962, p.85.
- [11] I.S.Shapiro, Phys.Rep. 35 (1978) 129.

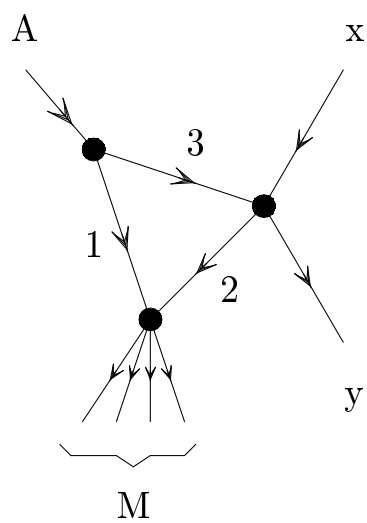


Figure 1: Typical triangle graph.

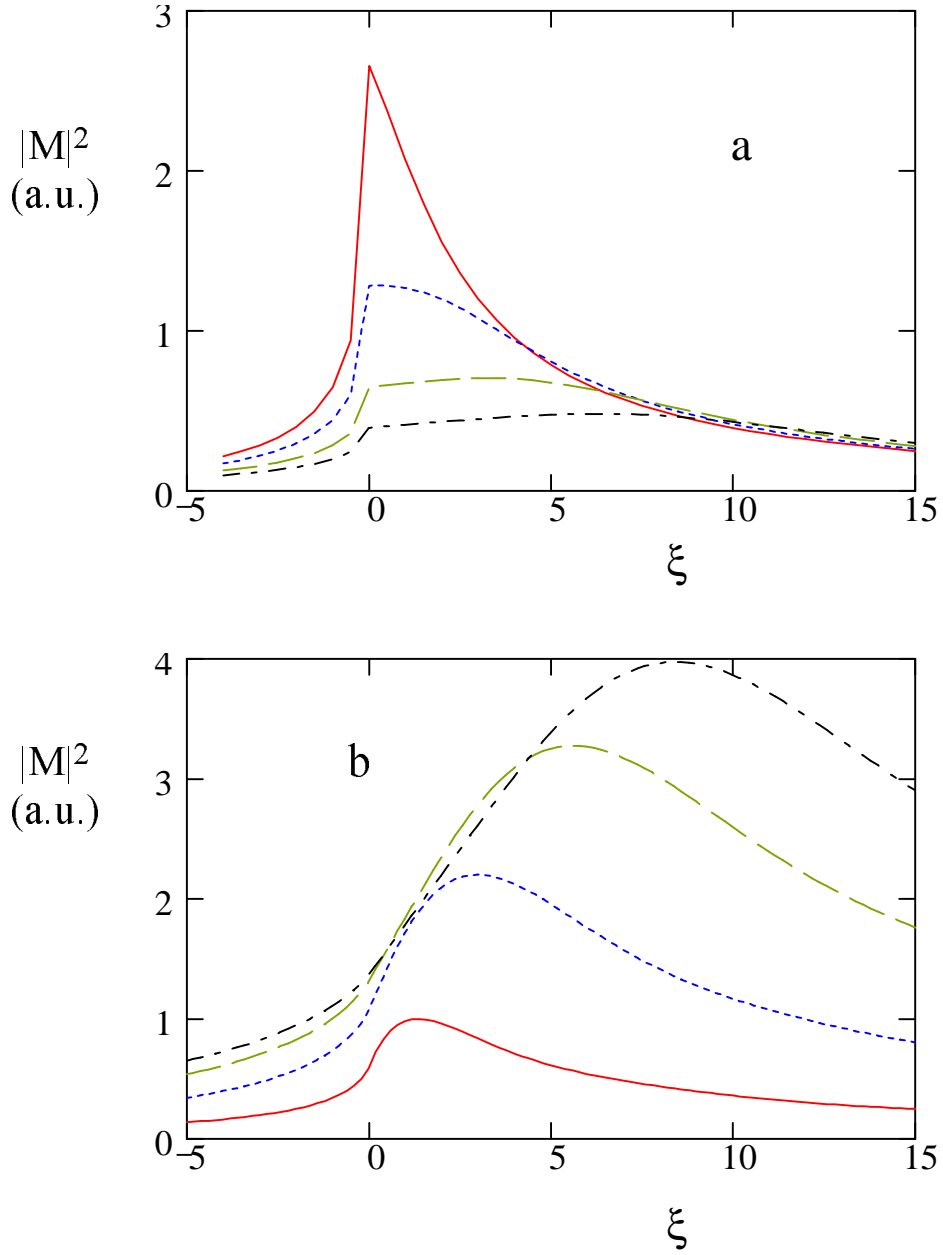


Figure 2:  $|\mathcal{M}|^2$  as a function of  $\xi$  for  $\lambda = 1$  (solid line), 3 (dotted line), 6 (dashed line), 9 (dash-dotted line) in the case of the deuteron with Paris wave function: a) for s-wave lower vertex, b) for p-wave lower vertex.

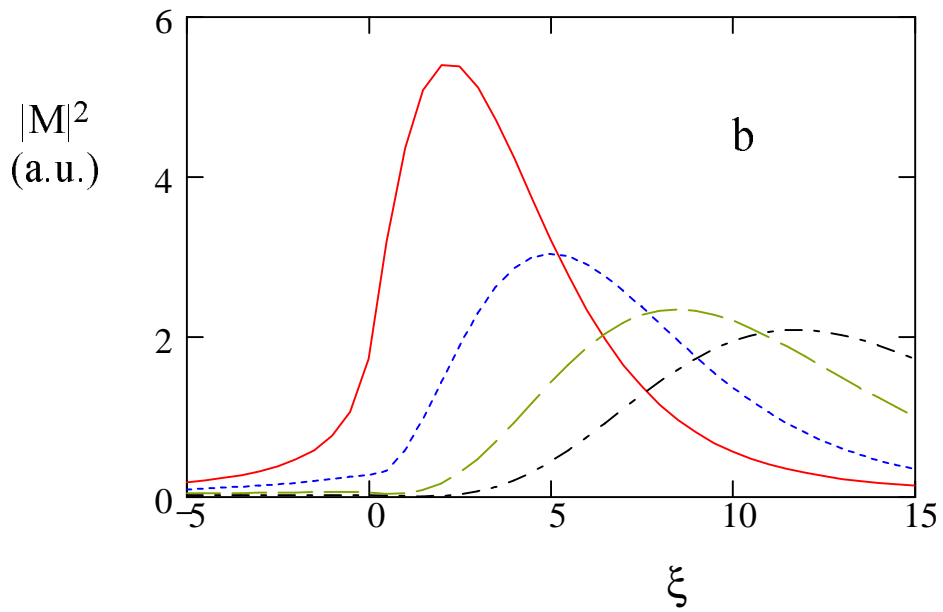
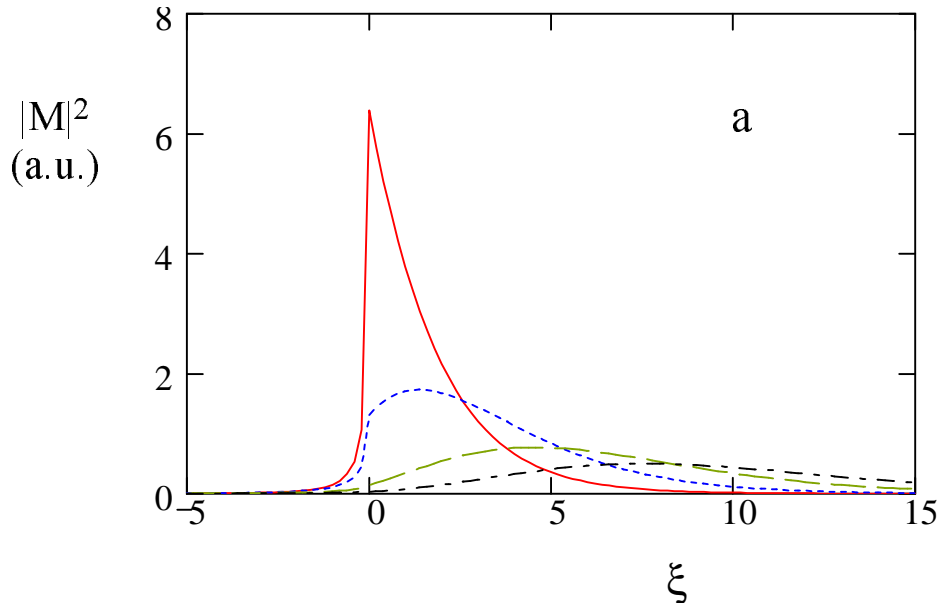


Figure 3: The same as in Fig.2 for p-wave nuclear function in the Gauss parametrization: a) for s-wave lower vertex, b) for p-wave lower vertex.